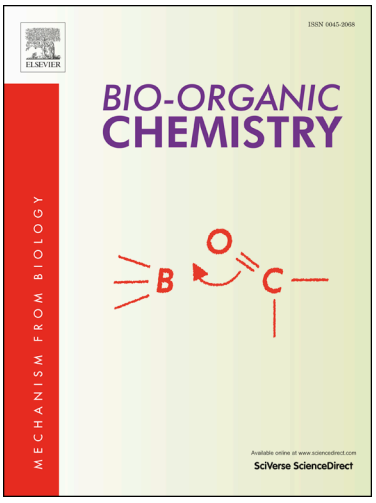

Design, Synthesis of Novel Azolyl Flavonoids and Their Protein Tyrosine Phosphatase-1B Inhibitory Activities

Ling Zhang, Yu Ge, Hao Ming Song, Qing Ming Wang, Cheng-He Zhou

PII: S0045-2068(18)30306-7
DOI: https://doi.org/10.1016/j.bioorg.2018.06.008
Reference: YBIOO 2388

To appear in: *Bioorganic Chemistry*

Received Date: 30 March 2018
Revised Date: 30 May 2018
Accepted Date: 3 June 2018

Please cite this article as: L. Zhang, Y. Ge, H. Ming Song, Q. Ming Wang, C-H. Zhou, Design, Synthesis of Novel Azolyl Flavonoids and Their Protein Tyrosine Phosphatase-1B Inhibitory Activities, *Bioorganic Chemistry* (2018), doi: https://doi.org/10.1016/j.bioorg.2018.06.008

Title page

Title:

Design, Synthesis of Novel Azolyl Flavonoids and Their Protein Tyrosine Phosphatase-1B Inhibitory Activities

Author names and affiliations:

Ling Zhang[1,*], Yu Ge[1], Hao Ming Song[1], Qing Ming Wang[1,*] and Cheng-He Zhou[2]

[1,*] *School of Pharmacy, Yancheng Teachers' University, Yancheng, Jiangsu 224051, People's Republic of China*

[2] *Laboratory of Bioorganic & Medicinal Chemistry, School of Chemistry and Chemical Engineering, Southwest University, Chongqing, 400715, P.R. China*

Tel.: 0515-88258905

E-mail: zling891613@163.com (Ling Zhang), wangqm@yctu.edu.cn (Qing Ming Wang)

Abstract:

A series of azolyl flavonoids were synthesized and characterized by NMR, IR, MS and HRMS spectra. All the newly prepared compounds were screened for their potential protein tyrosine phosphatase inhibitory activities. Bioactive assay manifested that most of the azolyl flavonoids exhibited good protein phosphatase 1B (PTP1B) inhibitory activities. Especially, triazolyl flavonoid **6a** displayed the best inhibitory activity (IC_{50} = 1.6 μM) with 9.9-fold selectivity for PTP1B over the closely related T-cell protein tyrosine phosphatase (TCPTP). Cell viability assays indicated **6a** has lower cytotoxicity. Molecular modeling and dynamics studies revealed the reason of selectivity for PTP1B over TCPTP. Quantum chemical studies were carried out on these compounds to understand the structural features essential for activity.

***Keywords*:**

Flavonoid; Azole; Protein tyrosine phosphatase; Selectivity; Cell viability

1. Introduction

Protein tyrosine phosphatases (PTPs) play an important role in modulation several cellular signal transduction pathways and catalysis protein tyrosine dephosphorylation [1]. Dysregulation of PTPs activities lead to the pathogenesis of many human diseases such as obesity, autoimmune disorders, cancers and diabetes [2]. Protein tyrosine phosphatases 1B (PTP1B), a key member of the PTP family, could regulate the insulin sensitivity and act by directly inactivating insulin receptor (IR) through dephosphorylation tyrosine residues in the regulatory domain. Insulin exerts an important effect in glucose uptake. Resistance of insulin results in reduced glucose intake and increased hepatic glucose output, which led to the increase of the blood glucose level [3]. A number of synthetic PTP1B inhibitors have been discovered [4-6]. Compound **1** was a classic PTP1B inhibitor (IC_{50} = 32 nM) designed on the basis of catalytic pocket characteristics and demonstrated modest caco-2 permeability (0.4×10^{-6} cm/s), but without selectivity (Figure 1). Compound **2** derived from natural products has also been proved to be active against PTP1B with micromolar level of activity (IC_{50} = 2.42 μM), however, the selectivity or membrane permeability was not further reported [7]. PTP inhibitors especially that can inhibit the particular PTP with good permeability received much attention [8].

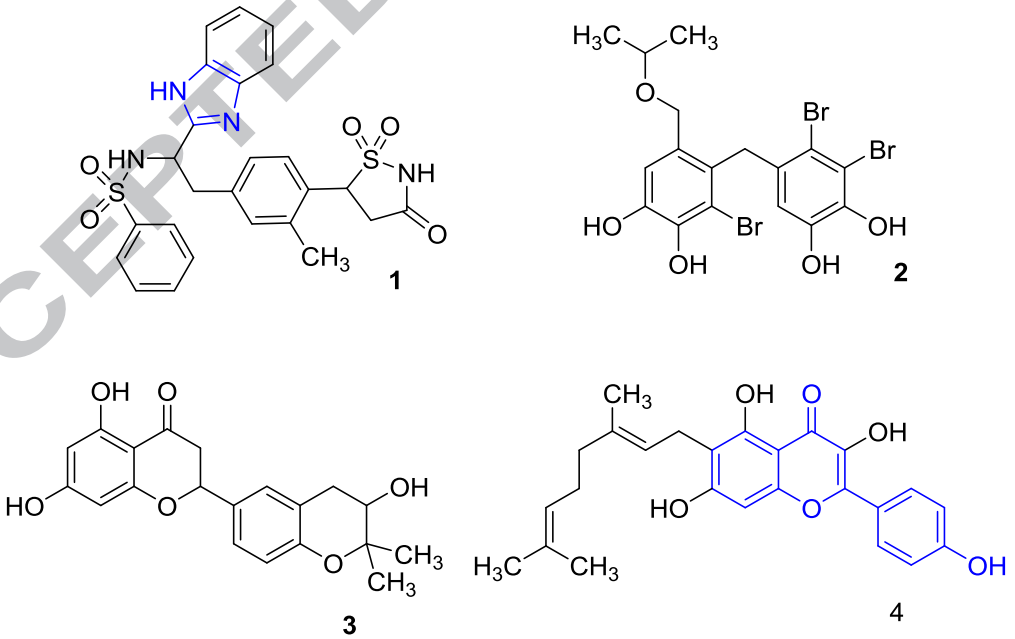

Fig. 1 Some reported PTP1B inhibitors

Flavonoids, a type of plant phenolic compounds, are widely found in nature with large potentiality in the

treatment of cancer, car-diovascular disease and neurodegenerative disorders. Recently, these natural flavones have drawn special attention as they are found to be good PTP1B inhibitors with low toxicity and high hypoglycemic effects [9]. It has disclosed that they could inhibit PTP1B activity in a non-competitive way different to the traditional drugs [10]. More and more flavonoids received much attention due to their unique properties in the inhibition of PTP1B (Figure 1).

Azoles (thiazoles, oxazoles, carbazoles, imidazoles, benz-imidazoles, triazoles, tetrazoles etc) are an important type of nitrogen heterocycles with aromaticity and electron rich properties. The special structure enables their derivatives to easily bind with the enzymes and receptors in organisms through noncovalent interactions such as coordination and hydrogen bonds, thereby giving them various medicinal applications. Recently, research has established that the introduction of nitrogen-containing heterocyclic moieties into the flavonoid backbone can improve bioactivity [11-14]. Especially, it reported that presence of azole ring is beneficial to improve the PTP1B inhibitory activity [15,16]. However, to the best of our knowledge, azolyl flavonoids have been rarely reported. In view of the above observations herein we incorporated different azole fragments into the O-7 position of flavonoid to generate a novel class of azolyl flavonoids. It evidenced that alkyl linkers can modulate physico-chemical properties and thus improve biological potency [17]. With the aim of better understanding structure–activity relationships and increasing flexibility, different lengths of alkyl chains were introduced into the target compounds to investigate the influence of linkers on bioactivities.

The designed structures of this series of novel azolyl flavonoids are shown in Scheme 1. All the newly synthesized compounds were characterized by spectral analysis and evaluated for their inhibition of PTP1B *in vitro*. Molecular modeling, molecular dynamics, energies and plots of HOMO and LUMO, and plots of MEP were also investigated by quantum chemical calculation to understand the structural features essential for activity.

2 Results and discussion

2.1. Chemistry

The target azolyl flavonoids were synthesized according to the synthetic route outlined in Scheme 1. Condensation of 1,3-benzenediol with chloro-acetonitrile in the presence of $ZnCl_2$ in ether was followed by hydrolysis in water and produced ketone **2** in 86% yield. The resulting **2** was reacted with benzaldehyde in ethanol with 10% NaOH, was followed by acidification with aqueous HCl to afford intermediate **3** in

satisfactory yields [18]. Compound **3** was then further treated with alkyl dibromides in acetone using potassium carbonate as base to afford bromides **4a-b** with yields of 50–76% [19]. The target azolyl flavonoids **5a–d**, **6a–d** and **7a–b** were conveniently and efficiently obtained in 50–67% yields by the reaction of bromides **4a–b** respectively with 2-methyl-5-nitroimidazole, 4-nitroimidazole, triazole, tetrazole or imidazole-thiol in acetonitrile at 50℃ in the presence of potassium carbonate as base. The target new compounds were confirmed by ^{1}H NMR, ^{13}C NMR, IR, MS and HRMS spectra.

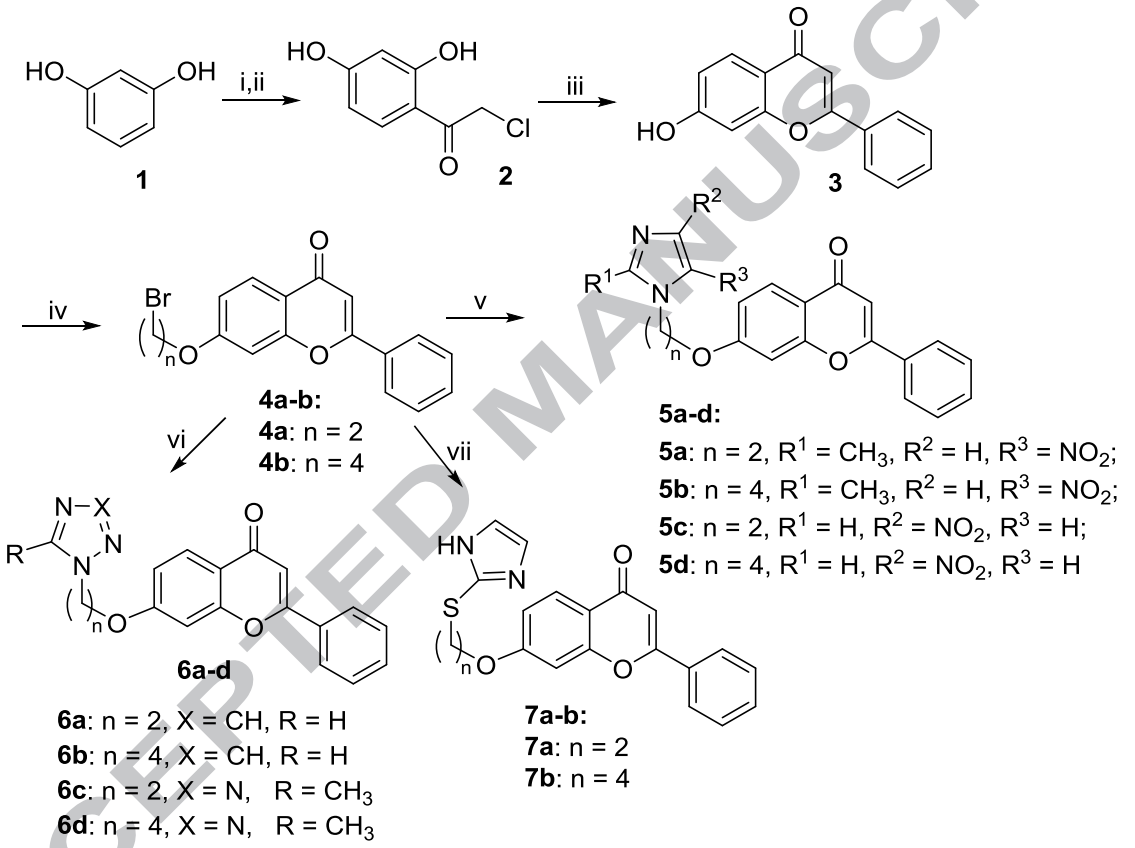

Scheme 1 Synthetic routes of azolyl flavonoids. Reagents and conditions: (i) $ClCH_2CN$, EtOEt, HCl (g), 0℃; (ii) 1 mol/L HCl, H_2O, reflux; (iii) benzaldehyde, 10%NaOH, rt, EtOH; (iv) alkyl dibromides, K_2CO_3, acetone, 50 ºC; (v) 2-methyl-5-nitroimidazole or 4-nitroimidazole, K_2CO_3, acetonitrile, 50 ºC; (vi) triazole or 5-methyl tetrazole, K_2CO_3, acetonitrile, 50 ºC; (vii) imidazole-thiol, K_2CO_3, acetonitrile, 50 ºC.

2.2. Biological evaluation

2.2.1. Inhibition of phosphatases

The obtained results as depicted in Table 1 revealed that azolyl flavonoids **5a–d**, **6a–d** and **7a–b** could effectively inhibit the PTP1B activity with IC_{50} values of 1.6–15.1 μmol/L. Table 1 showed the significant

effects of the types of azole rings and alkyl chain lengths on biological activity. Generally, long-chain alkyl possessed less inhibitory activities than short-chain derivatives. The long alkyl ones with higher lipophilicity in these compounds might make them unfavourable to be delivered to the binding sites.

Among them, triazolyl functionalized compound **6a** gave the best inhibitory activity against PTP1B with MIC values of 1.6 μmol/L. The substitution of triazole with 2-methyl-5-nitroimidazole, 4-nitroimidazole, 5-methyl tetrazole or thiol-imidazole group which yielded compounds **5a**, **5c**, **6c** and **7a** resulted in relatively lower activity. These results revealed that existence of triazole moiety in this series of azolyl flavonoids should be of special importance in the PTP1B Inhibition profiles.

In view of above discussion, the anti-PTP1B efficacies should be closely related to azole ring and alkyl chain lengths to some extent. For this serial compounds, azole moieties contributed to the anti-PTP1B activities in the order of triazole > imidazole-thiol > 2-methyl-5-nitroimidazole > 4-nitroimidazole > 5-methyl tetrazole derivatives. The triazolyl group was more helpful for increasing anti-PTP1B efficacy in comparison to other azolyl ones.

Table 1 Inhibitory activities against PTP1B (μmol/L)

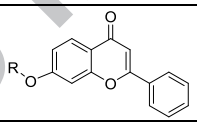

Compds	R	IC_{50}	Compds	R	IC_{50}
5a		4.0±1.7	**6b**		3.6±0.4
5b	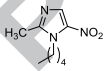	6.9±1.3	**6c**		7.9±0.3
5c		5.0±1.2	**6d**		15.1±0.9
5d		7.0±1.1	**7a**		3.0±0.04
6a		1.6±0.9	**7b**		3.9±0.9

Further, the selectivity of the **6a** was determined by measuring their inhibitory activity against a panel of several phosphatases including TCPTP, PTP-MEG2 and SHP-2. The IC_{50} values of inhibitor **6a** against the phosphatases, and the selectivity ratios were shown in Table 2. Compound **6a** showed no activity against PTP-MEG2, and only exhibited moderate activity for SHP-2. Compound **6a** was selective for PTP1B over

PTP-MEG2 and SHP2. Notably, compound **6a** showed 9.9-fold selectivity for PTP1B over TCPTP, since TCPTP was the most closely related to PTP1B in phosphatase.

Table 2 Inhibition of phosphatases by inhibitor **6a**

Compd	IC_{50}(μM)				
	PTP1B	TCPTP	PTP-MEG2	SHP-2	Selective
6a	1.6	15.8	NA	19.8	9.9

[a] NA: no activity
[b] Selective: IC_{50}(TCPTP)/IC_{50}(PTP1B)
[c] Abbreviations: PTP1B, protein tyrosine phosphatase 1B; TCPTP, T-cell protein tyrosine phosphatase; PTP-MEG2, megakaryocyte protein tyrosine phosphatase; SHP-2, src homology phosphatase 2.

2.2.2. Kinetic analysis of PTP1B inhibition

A kinetic analysis of compound **6a** was then conducted using *p*-NPP as the small-molecule substrate in a continuously monitored colorimetric assay. Four different concentrations of the substrate *p*-NPP (1, 2, 4, 8 μM) were used in the steady state kinetics assays. Figure 2 shows the Lineweavere Burk double-reciprocal plot of the kinetics data in the presence of various concentrations of compound **6a**. It appears that the lines converged at an intersection on the y-axis above the x-axis, implying a competitive inhibition mode versus *p*-NPP.

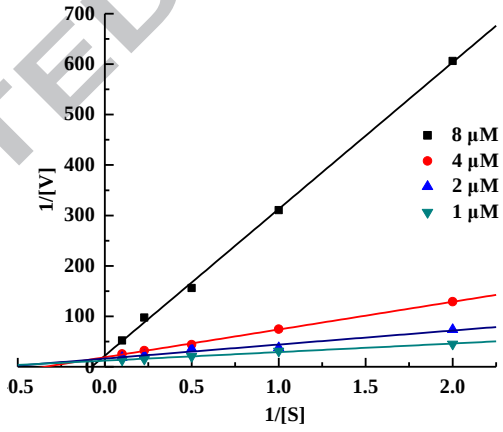

Fig. 2 Compound **6a** is a classical competitive inhibitor

*2.3. The influence of **6a** on cell viability*

The effect of **6a** on cell viability of HEK293 (human embryonic kidney 293) cells was further tested by Cell Counting Kit-8 (CCK8) method. As shown in Figure 3, compound **6a** showed relative low toxicity to normal human embryonic kidney cells at high concentration, and the IC_{50} value was 106 μg/mL. The results demonstrated **6a** has lower cytotoxicity.

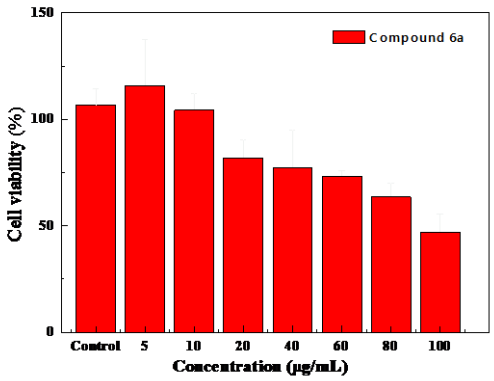

Fig. 3 Relative cell viabilities of compound **6a** in HEK293 cells.

2.4. Molecular modeling

To rationalize the observed PTP1B inhibitory activity of the target flavonoids, active site-docking simulations of the compounds were performed to calculate their lowest-energy conformations (Figure 4 and Figure 5). The crystal structure data (PTP1B) were obtained from the protein data bank (PDB code: 1G1H). Target compound **6a** was selected to dock with the PTP1B.

According to the docking evaluation, the most active **6a** showed high binding energy (E = -8.69 kJ/mol) with PTP1B (Figure 4). The docking result of compound **6a** with PTP1B might rationalize the possible inhibitory mechanism. The 1-position and 2-position nitrogen atoms of the triazole moiety could form hydrogen bonds with residue ARG-221 of PTP1B with length of 2.5 and 2.1 Å respectively, which indicated the necessity of triazole moiety for the increased bioactivity. The oxygen atom on the alkoxy group could form hydrogen bonds with the residue ARG-221 and SER-216 at the same time, with the distance of 1.9 and 2.3 Å, respectively. The oxygen atom on the carbonyl could also form hydrogen bond with the residue LYS-120 at the distance of 2.1 Å. Furthermore, besides hydrogen bonds, the compound–PTP1B enzyme complex could be stabilized by several hydrophobic interactions (Figure 5). This cooperative binding might be beneficial to stabilize the compound–PTP1B enzyme complex, which might be responsible for the good inhibitory efficacy of compound **6a** against PTP1B.

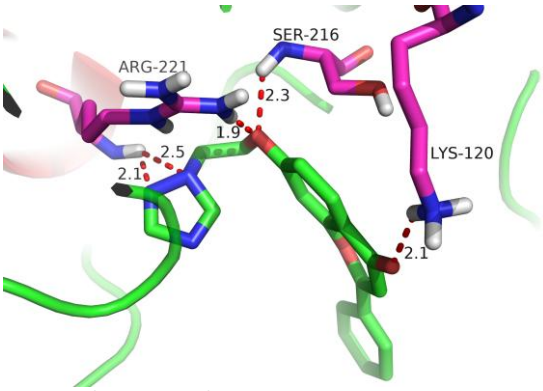

Fig. 4 Three-dimensional conformation of compound **6a** docked onto the active site of PTP1B.

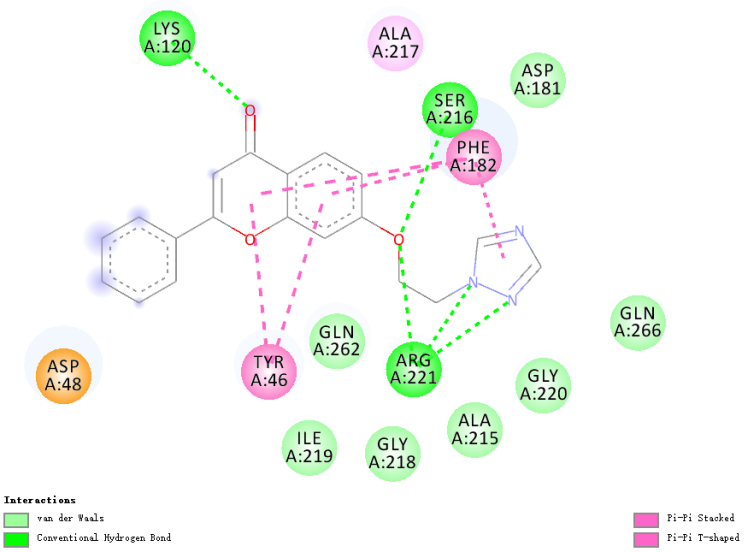

Fig. 5 Two-dimensional conformation of compound **6a** docked onto the active site of PTP1B.

In order to explain the selectivity of inhibitor **6a**, the binding mode of compound **6a** with TCPTP (PDB code: 1L8K) was performed. Compound **6a** showed relatively lower binding energy (E = -7.1 kJ/mol) than PTP1B. Some main interactions between inhibitor **6a** and the receptor can be observed in Figure 6. Only the 1-position nitrogen atom of the triazole moiety and oxygen atom of this molecule formed hydrogen bonding with amino acid residues Ser217 and Arg222 with length of 2.6 Å and 2.2 Å respectively, that was different with the binding pattern of **6a** with PTP1B (Figure 4 and 5).

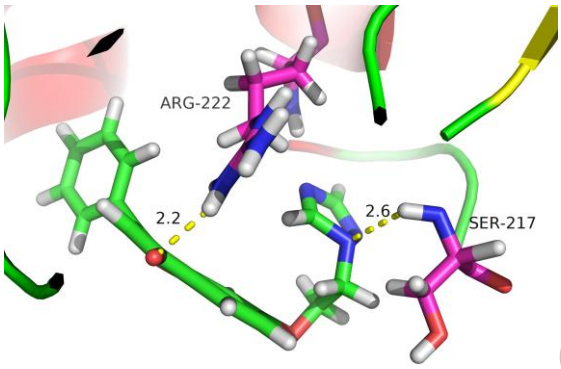

Fig. 6 Three-dimensional conformation of compound **6a** docked onto the active site of TCPTP.

2.5. Analysis of the Dynamics Studies

A continuous effort was made to explain the selectivity of inhibitor **6a** by performing molecular dynamics (MD) simulations.

The interaction of the protein with ligands is a dynamic process different with static process of molecular docking. The dynamic process of results in a lower binding energy of the complex and a more stable complex, and could be displayed by MD simulation. Analysis of the root-mean-squared deviation (RMSD) values indicates that the RMSDs of both systems reached equilibration and oscillated around an average value after 20 and 10 ns simulation, respectively. The backbone RMSD value of PTP1B was lower than that of TCPTP, which suggested that the PTP1B/**6a** was more stable than TCPTP/**6a** in 50 ns MD simulation (Figure 7). All these observations revealed that the interaction between **6a** and PTP1B was more potent and stable than that between **6a** and TCPTP. That may be the reason, at least in part, why compound **6a** displayed obvious selectivity for PTP1B over TCPTP.

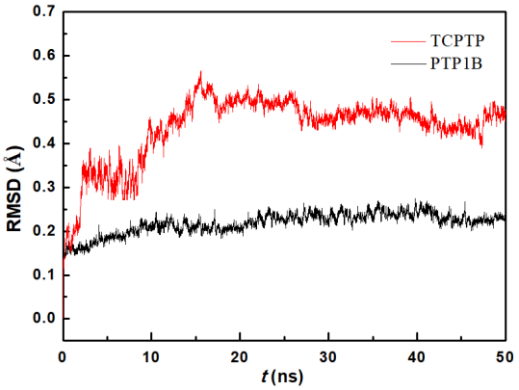

Fig. 7 Time dependence of root-mean-square deviations (RMSD's) for **6a** bound with TCPTP (1L8K, in red) and PTP1B (1G1H, in black)

The integrity of the protein was analyzed by plotting Rg values against time. The Rg describes the overall spread of the molecule and is defined as the root-mean-square distance of the collection of atoms from their common center of gravity. In the present MD studies, we determined the Rg values of free PTP1B and PTP1B-compound **6a** complex as shown in Figure 8. The Rg values were stabilized at about 35 ns, indicating that the MD simulation achieved equilibrium after 50 ns. Initially, the Rg values of free PTP1B and PTP1B-compound **6a** complex were 1.92 nm. The free PTP1B and PTP1B-compound **6a** complex were stabilized at 1.91±0.01 and 1.89±0.01 respectively. These results suggest that the Rg value marginally decreased upon binding of compound **6a**. The above results emphasize that the compound **6a** bind to PTP1B in MD simulations due to a change in the microenvironment of PTP1B which leads to the conformational changes in the protein. Thus, the MD simulation data clearly showed that PTP1B-compound **6a** complex was stabilized due to conformational rearrangements.

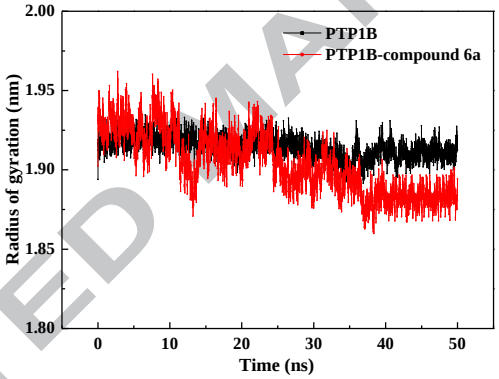

Fig. 8 Time evolution of the radius of gyration values during 50 ns of MD simulation of PTP1B and PTP1B-compound **6a** complex.

The local protein flexibility was investigated by calculated RMSF values of free PTP1B and PTP1B-compound **6a** complex, which were plotted against residue numbers on a 50 ns trajectory and distinctly indicate that the flexibility of PTP1B is more than PTP1B-compound **6a** complex. The higher flexibility of PTP1B is mainly because of interactions of compound **6a** with the target protein, PTP1B. This inherent flexibility of PTP1B is likely to play an important role in the ligand binding (Figure 9). The analysis provides an indication that PTP1B binding site interacts clearly with compound **6a** through remodeling of the compound **6a** to the specific sites of PTP1B, which results in structural alteration of the protein.

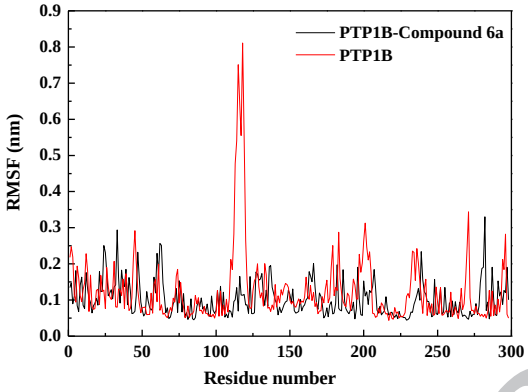

Fig. 9 RMSF analysis of complex structure during molecular dynamics simulation

2.6. Molecular orbital calculation

Electronic effects were shown to be related with biological activity of drugs [20]. At the molecular level, the frontier molecular orbitals (FMO) controlled the reactivity of a molecule, namely the highest occupied molecular orbital (HOMO) and the lowest unoccupied molecular orbital (LUMO) and they exerted important effect in intermolecular interactions [21]. The extents of these stabilizing interactions in inversely correlation with the energy gap between the interacting orbitals. Higher HOMO energy and lower LUMO energy lead to larger stabilizing interactions, favoring for binding with the receptor. Hence, the orbital energies of both HOMO and LUMO and their gaps were calculated for compounds **6a** and **6d** as shown in Table 3. The HOMO-LUMO energy gap value supports the intramolecular charge-transfer interactions within the molecule. It was noteworthy that the most active compound **6a** gave the lowest energy gap (Δε) of 10.85 eV.

Table 3 Energies of both HOMO and LUMO and their gaps (in eV) calculated for compounds **6a** and **6d**.

Compds	εHOMO (eV)	εLUMO (eV)	Δε (eV)
6a	-8.80	2.05	10.85
6d	-9.17	1.96	11.13

The plots of the HOMOs and LUMOs of **6a** and **6d** were also obtained successfully to further analyze the main atomic contributions for these orbitals. The results presented in Table 4 demonstrated that the electron charge cloud is located at the flavonoid ring in highest occupied molecular orbital (HOMO) of **6a** and **6d** which indicated that active sites might be at this ring and biological interactions could take place between positively charged molecules and these sites. It was also found that azole ring and substituents on the ring did not contribute directly to HOMOs which manifested these groups might be primarily used to modulate the physicochemical properties. Moreover, the LUMOs of these molecules were also mainly centered at the flavonoid ring in which nucleophilic attacks might be favorable.

Table 4 Plots of the HOMO and LUMO of compounds **6a** and **6d**

Compds	HOMO	LUMO
6a	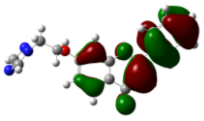	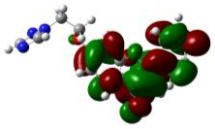
6d	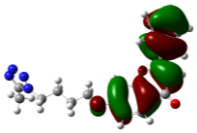	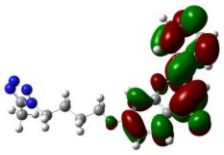

2.7. Molecular electrostatic potentials

In order to deeply understand the lower inhibitory activities of compound **6d** together with the higher inhibitory activity of **6a**, molecular electrostatic potentials (MEPs) had been proceeded to check the similarities and differences in electrostatic binding characteristic of the surface of the molecules (Table 5). Comparison of the electrostatic maps of **6a** and **6d** revealed that compound **6a** had an increased positive charge regions (blue region) located on the triazole ring probably due to influence of the aromatic substituent, and **6a** also possessed more negative charge regions (red region) on the oxygen atom of flavonoid ring. It might indicate compound **6a** had strong capability of interacting with polar residues of enzymes or receptors to form hydrogen bond through triazole ring and the oxygen atom of flavonoid ring. This was consistent with the binding mode obtained from above docking study.

Table 5 Molecular electrostatic potentials (MEPs) of compounds **6a** and **6d** showing the most positive potential (deepest blue color), the most negative potential (deepest red color), and the intermediate potential (intermediate shades) regions

Compds	Molecular electrostatic potentials
	
6a	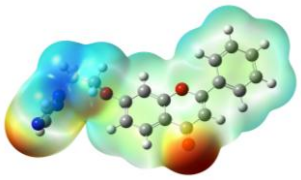

6d	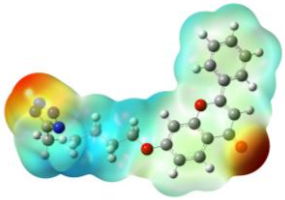

3 Conclusion

In conclusion, a series of azolyl flavonoids were successfully synthesized by a convenient and efficient procedure. Their structures were confirmed by ^{1}H NMR, ^{13}C NMR, MS, IR and HRMS spectra. The *in vitro* protein tyrosine phosphatase inhibition evaluation revealed that most of azolyl flavonoids exhibited good protein phosphatase 1B (PTP1B) inhibitory activities at the micromolar range. The most active compound **6a** with IC_{50} values of 1.6 μM displayed 9.9-fold selectivity over TCPTP. Molecular modeling studies indicated that the triazole ring played an important role in the interaction of inhibitor with PTP1B. The MD studies revealed that the PTP1B/**6a** complex was more stable than TCPTP/**6a**, which was the potent proof for observed 9.9-fold selectivity of **6a** for PTP1B over TCPTP, although TCPTP and PTP1B shared high degree of homology in catalytic site. These results provided further evidence that azolyl flavonoids can be potent inhibitors of PTP1B. Further studies on these compounds in cell permeability, selectivity and cellular activity would be necessary to provide PTP1B inhibitors suitable for *in vivo* proof of animal studies in diabetes.

4 Experimental protocols

4.1 General methods

Melting points were recorded on X-6 melting point apparatus and uncorrected. TLC analysis was done using pre-coated silica gel plates. FT-IR spectra were carried out on Bruker RFS100/S spectrophotometer (Bio-Rad, Cambridge, MA, USA) using KBr pellets in the 400–4000 cm^{-1} range. NMR spectra were recorded on a Bruker AV 300 and 600 spectrometer using TMS as an internal standard. The chemical shifts were reported in parts per million (ppm), the coupling constants (*J*) were expressed in hertz (Hz) and signals were described as singlet (s), doublet (d), triplet (t), as well as multiplet (m). The mass spectra were recorded on LCMS-2010A and the high-resolution mass spectra (HRMS) were recorded on an IonSpec FT-ICR mass spectrometer with ESI resource. All other chemicals (Shanghai Titan Technology Co., Ltd) and solvents were commercially available, and were used without further purification.

4.2 Synthesis of azolyl flavonoids

*4.2.1. Synthesis of 7-(2-(2-methyl-5-nitro-1H-imidazol-1-yl)ethoxy)-2-phenyl-4H-chromen-4-one (**5a**)*

A mixture of 2-methyl-5-nitro-1H-imidazole (0.76 g, 6 mmol) and potassium carbonate (0.83 g, 6 mmol) in CH_3CN (20 mL) was stirred for 1 h at room temperature, and then compound **4a** (1.73 g, 5 mmol) was added. The resulting mixture was stirred at 50 ℃ for 16 h (monitored by TLC, eluent, petroleum ether/ethylacetate, 3/1, V/V). The solvents were evaporated under reduced pressure, and the residue was treated with water (50 mL) and extracted with chloroform (3×50 mL). The organic layers were combined, dried with anhydrous Na_2SO_4, and concentrated under reduced pressure. The crude product was purified via silica gel column chromatography (eluent, petroleum ether/ethylacetate, 5/1, V/V) to afford compound **5a** (1.25 g) as white power. Yield: 64%; mp: 199–200 ℃; IR (KBr, cm^{-1}) ν: 3052 (Ar–H), 2965 (CH_3), 1811 (aromatic frame), 1700 (C=O), 1619, 1578 (aromatic frame); ^{1}H NMR (400 MHz, DMSO-d_6) δ: 8.31 (s, 1H, imidazole 4-H), 8.01–7.82 (m, 2H, Ph-2,6-2*H*), 7.54 (d, *J* = 7.5 Hz, 1H, flavone-5-*H*), 7.50–7.42 (m, 3H, Ph-3,4,5-3*H*), 7.22 (d, *J* = 2.3 Hz, 1H, flavone-3-*H*), 6.83 (s, 1H, flavone-6-*H*), 6.72 (dd, *J* = 7.5, 2.0 Hz, 1H, flavone-8-*H*), 4.22 (q, *J* = 4.1 Hz, 2H, N-CH_2), 4.00 (dd, *J* = 10.2, 5.1 Hz, 2H, O-CH_2), 2.33 (s, 3H, CH_3) ppm; ^{13}C NMR (101 MHz, DMSO-d_6) δ: 181.1, 167.2, 165.3, 155.1, 147.8, 145.5, 132.2, 131.6, 131.0, 130.4, 129.6, 128.2, 126.6, 115.3, 112.8, 99.5, 66.5, 49.4, 27.1, 20.1 ppm; MS (m/z): 392 $[M+H]^+$; HRMS (TOF) calcd for $C_{21}H_{17}N_3O_5$: $[M+H]^+$, 392.1246; found, 392.1248.

*4.2.2. Synthesis of 7-(4-(2-methyl-5-nitro-1H-imidazol-1-yl)butoxy)-2-phenyl-4H-chromen-4-one (**5b**)*

Compound **5b** was prepared according to the experimental procedure for compound **5a**. White solid; Yield: 62%; mp: 202–203 ℃; IR (KBr, cm^{-1}) ν: 3049 (Ar–H), 2988 (CH_3), 1800 (aromatic frame), 1726 (C=O), 1625, 1538, 1462 (aromatic frame); ^{1}H NMR (400 MHz, DMSO-d_6) δ: 8.23 (s, 1H, imidazole 4-H), 8.22–7.95 (m, 2H, Ph-2,6-2*H*), 7.68 (d, *J* = 8.1 Hz, 1H, flavone-5-*H*), 7.52–7.41 (m, 3H, Ph-3,4,5-3*H*), 7.19 (d, *J* = 2.0 Hz, 1H, flavone-3-*H*), 6.89 (s, 1H, flavone-6-*H*), 6.79 (dd, *J* = 8.2, 3.0 Hz, 1H, flavone-8-*H*), 5.11–5.00 (m, 2H, N-CH_2), 4.77–4.64 (m, 2H, O-CH_2), 2.40 (s, 3H, CH_3), 1.65 (dt, 4H, J = 14.2, 7.1 Hz, CH_2CH_2) ppm; ^{13}C NMR (101 MHz, DMSO-d_6) δ: 182.5, 169.5–168.1, 167.0, 164.1–163.9, 148.5, 133.7–132.2, 131.3, 128.5, 126.2, 113.8, 111.6, 98.3, 66.6, 52.2, 10.6 ppm; MS (m/z): 420 $[M+H]^+$; HRMS (TOF) calcd for $C_{23}H_{21}N_3O_5$: $[M+H]^+$, 420.1559; found, 420.1557.

*4.2.3. Synthesis of 7-(2-(4-nitro-1H-imidazol-1-yl)ethoxy)-2-phenyl-4H-chromen-4-one (**5c**)*

Compound **5c** was prepared according to the experimental procedure for compound **5a**. White power. Yield: 69%; mp: 190–191 ℃; IR (KBr, cm^{-1}) ν: 3053 (Ar–H), 1811 (aromatic frame), 1726 (C=O), 1648, 1574 (aromatic frame); ^{1}H NMR (400 MHz, DMSO-d_6) δ: 8.07 (s, 1H, imidazole 2-*H*), 7.82 (s, 1H, imidazole 5-*H*),

8.05–7.96 (m, 2H, Ph-2,6-2*H*), 7.65 (d, *J* = 8.5 Hz, 1H, flavone-5-*H*), 7.52–7.41 (m, 3H, Ph-3,4,5-3*H*), 7.24 (d, *J* = 2.6 Hz, 1H, flavone-3-*H*), 6.87 (s, 1H, flavone-6-*H*), 6.80 (dd, *J* = 8.3, 2.6 Hz, 1H, flavone-8-*H*), 4.52 (q, *J* = 4.2 Hz, 2H, N-CH_2), 4.46 (dd, *J* = 10.1, 5.1 Hz, 2H, O-CH_2) ppm; ^{13}C NMR (101 MHz, DMSO-d_6) δ: 181.7, 167.2, 165.4, 153.2, 148.4, 146.3, 133.5, 132.2, 131.1, 130.2, 129.3, 128.2, 126.0, 115.5, 114.5, 112.2, 98.6, 63.1, 41.2 ppm; MS (m/z): 378 $[M+H]^+$; HRMS (TOF) calcd for $C_{20}H_{15}N_3O_5$: $[M+H]^+$, 378.1090; found, 378.1096.

*4.2.4. Synthesis of 7-(3-(4-nitro-1H-imidazol-1-yl)propoxy)-2-phenyl-4H-chromen-4-one (**5d**)*

Compound **5d** was prepared according to the experimental procedure for compound **5a**. White solid; Yield: 60%; mp: 201–202 ℃; IR (KBr, cm^{-1}) ν: 3036 (Ar–H), 1824 (aromatic frame), 1744 (C=O), 1624, 1535, 1461 (aromatic frame); ^{1}H NMR (400 MHz, DMSO-d_6) δ: 8.24–8.19 (m, 2H, Ph-2,6-2*H*), 8.11 (s, 1H, imidazole 2-*H*), 8.02 (s, 1H, imidazole 5-*H*), 7.58 (d, *J* = 7.4 Hz, 1H, flavone-5-*H*), 7.50–7.40 (m, 3H, Ph-3,4,5-3*H*), 7.22 (d, *J* = 2.5 Hz, 1H, flavone-3-*H*), 6.91 (s, 1H, flavone-6-*H*), 6.76 (dd, *J* = 8.3, 3.5 Hz, 1H, flavone-8-*H*), 5.13–5.01 (m, 2H, N-CH_2), 4.82–4.68 (m, 2H, O-CH_2), 1.79–1.76 (m, 2H, CH_2CH_2), 1.72–1.68 (m, 2H, CH_2CH_2) ppm; ^{13}C NMR (101 MHz, DMSO-d_6) δ: 180.6, 168.9, 166.5, 165.2, 164.2, 148.5, 134.7, 132.3, 129.4, 125.3, 115.6, 112.7, 98.4, 67.1, 53.2, 20.6 ppm; MS (m/z): 392 $[M+H]^+$; HRMS (TOF) calcd for $C_{21}H_{17}N_3O_5$: $[M+H]^+$, 392.1246; found, 392.1240.

*4.2.5. Synthesis of 7-(2-(1H-1,2,4-triazol-1-yl)ethoxy)-2-phenyl-4H-chromen-4-one (**6a**)*

Compound **6a** was prepared according to the experimental procedure for compound **5a**. White power. Yield: 67%; mp: 185–186 ℃; IR (KBr, cm^{-1}) ν: 3061 (Ar–H), 1804 (aromatic frame), 1718 (C=O), 1617, 1571 (aromatic frame); ^{1}H NMR (400 MHz, DMSO-d_6) δ: 8.62 (s, 1H, triazole-5-*H*), 8.02 (s, 1H, triazole-3-*H*), 8.00–7.95 (m, 2H, Ph-2,6-2*H*), 7.69 (d, *J* = 8.6 Hz, 1H, flavone-5-*H*), 7.55–7.43 (m, 3H, Ph-3,4,5-3*H*), 7.21 (d, *J* = 2.1 Hz, 1H, flavone-3-*H*), 6.86 (s, 1H, flavone-6-*H*), 6.82 (dd, *J* = 8.6, 2.1 Hz, 1H, flavone-8-*H*), 4.66 (q, *J* = 4.6 Hz, 2H, N-CH_2), 4.55 (dd, *J* = 10.3, 5.3 Hz, 2H, O-CH_2) ppm; ^{13}C NMR (101 MHz, DMSO-d_6) δ: 182.1, 168.3, 166.3, 152.0, 147.6, 145.2, 132.4, 131.6, 131.2, 130.4, 129.5, 128.8, 126.1, 114.6, 113.4, 111.6, 98.4, 67.2, 48.4 ppm; MS (m/z): 334 $[M+H]^+$; HRMS (TOF) calcd for $C_{19}H_{15}N_3O_3$: $[M+H]^+$, 334.1192; found, 334.1197.

*4.2.6. Synthesis of 7-(4-(1H-1,2,4-triazol-1-yl)butoxy)-2-phenyl-4H-chromen-4-one (**6b**)*

Compound **6b** was prepared according to the experimental procedure for compound **5a**. White power. Yield: 64%; mp: 190–191 ℃; IR (KBr, cm^{-1}) ν: 3034 (Ar–H), 1901 (aromatic frame), 1763 (C=O), 1625, 1598, 1575 (aromatic frame); ^{1}H NMR (400 MHz, DMSO-d_6) δ: 8.53 (s, 1H, triazole-5-*H*), 7.93 (s, 1H, triazole-3-*H*), 8.02–7.94 (m, 2H, Ph-2,6-2*H*), 7.53 (d, *J* = 8.5 Hz, 1H, flavone-5-*H*), 7.50–7.44 (m, 3H, Ph-3,4,5-3*H*), 7.24 (d, *J* = 2.3 Hz, 1H, flavone-3-*H*), 6.85 (s, 1H, flavone-6-*H*), 6.79 (dd, *J* = 8.5, 2.2 Hz, 1H, flavone-8-*H*), 4.66 (q, *J* =

4.6 Hz, 2H, N-CH_2), 4.55 (dd, *J* = 10.3, 5.3 Hz, 2H, O-CH_2), 2.01 (m, 2H, CH_2), 1.81 (m, 2H, CH_2) ppm; ^{13}C NMR (101 MHz, DMSO-d_6) δ: 182.1, 168.3, 166.3, 152.0, 147.6, 145.2, 132.4, 131.8, 131.4, 130.2, 129.1, 128.2, 125.4, 115.5, 113.2, 110.4, 97.2, 63.1, 44.1, 13.6, 12.1 ppm; MS (m/z): 362 $[M+H]^+$; HRMS (TOF) calcd for $C_{21}H_{19}N_3O_3$: $[M+H]^+$, 362.1505; found, 362.1509.

*4.2.7. Synthesis of 7-(2-(5-methyl-1H-tetrazol-1-yl)ethoxy)-2-phenyl-4H-chromen-4-one (**6c**)*

Compound **6c** was prepared according to the experimental procedure for compound **5a**. White solid; Yield: 64%; mp: 201–202 ℃; IR (KBr, cm^{-1}) ν: 3050 (Ar–H), 1805 (aromatic frame), 1716 (C=O), 1615, 1548, 1482 (aromatic frame); ^{1}H NMR (400 MHz, DMSO-d_6) δ: 8.01–7.95 (m, 2H, Ph-2,6-2*H*), 7.68 (d, *J* = 8.5 Hz, 1H, flavone-5-*H*), 7.54–7.46 (m, 3H, Ph-3,4,5-3*H*), 7.22 (d, *J* = 2.0 Hz, 1H, flavone-3-*H*), 6.87 (s, 1H, flavone-6-*H*), 6.79 (dd, *J* = 8.5, 2.1 Hz, 1H, flavone-8-*H*), 5.13–5.06 (m, 2H, N-CH_2), 4.76–4.69 (m, 2H, O-CH_2), 2.47 (s, 3H, CH_3) ppm; ^{13}C NMR (101 MHz, DMSO-d_6) δ: 182.3, 168.3–168.1, 166.0, 163.1–162.9, 147.6, 132.7–132.5, 131.5, 129.4, 126.1, 114.8, 111.5, 98.4, 66.7, 52.1, 10.9 ppm; MS (m/z): 349 $[M+H]^+$; HRMS (TOF) calcd for $C_{19}H_{16}N_4O_3$: $[M+H]^+$, 349.1301; found, 349.1308.

*4.2.8. Synthesis of 7-(4-(5-methyl-1H-tetrazol-1-yl)butoxy)-2-phenyl-4H-chromen-4-one (**6d**)*

Compound **6d** was prepared according to the experimental procedure for compound **5a**. White solid; Yield: 61%; mp: 204–205 ℃; IR (KBr, cm^{-1}) ν: 3044 (Ar–H), 1815 (aromatic frame), 1725 (C=O), 1634, 1557, 1455 (aromatic frame); ^{1}H NMR (400 MHz, DMSO-d_6) δ: 8.10–7.99 (m, 2H, Ph-2,6-2*H*), 7.59 (d, *J* = 8.5 Hz, 1H, flavone-5-*H*), 7.51–7.45 (m, 3H, Ph-3,4,5-3*H*), 7.19 (d, *J* = 3.2 Hz, 1H, flavone-3-*H*), 6.75 (s, 1H, flavone-6-*H*), 6.71 (dd, *J* = 8.3, 2.0 Hz, 1H, flavone-8-*H*), 5.16–5.08 (m, 2H, N-CH_2), 4.68–4.62 (m, 2H, O-CH_2), 2.31 (s, 3H, CH_3), 2.11 (m, 2H, CH_2), 1.93 (m, 2H, CH_2) ppm; ^{13}C NMR (101 MHz, DMSO-d_6) δ: 183.1, 169.0, 167.2, 164.9, 148.3, 133.6, 131.2, 129.5, 125.3, 114.6, 112.3, 98.5, 66.6, 53.1, 13.2, 10.9 ppm; MS (m/z): 376 $[M+H]^+$; HRMS (TOF) calcd for $C_{21}H_{20}N_4O_3$: $[M+H]^+$, 376.4160; found, 376.4162.

*4.2.9. Synthesis of 7-(2-((1H-imidazol-2-yl)thio)ethoxy)-2-phenyl-4H-chromen-4-one (**7a**)*

Compound **7a** was prepared according to the experimental procedure for compound **5a**. Yellow solid; Yield: 62%; mp: 191–192 ℃; IR (KBr, cm^{-1}) ν: 3458 (NH), 3060 (Ar–H), 1805 (aromatic frame), 1717 (C=O), 1614, 1546, 1481 (aromatic frame); ^{1}H NMR (400 MHz, DMSO-d_6) δ: 8.01–7.96 (m, 2H, Ph-2,6-2*H*), 7.69 (d, *J* = 8.6 Hz, 1H, flavone-5-*H*), 7.54–7.45 (m, 3H, Ph-3,4,5-3*H*), 7.28 (d, *J* = 1.1 Hz, 1H, flavone-3-*H*), 7.22 (d, *J* = 2.0 Hz, 1H, imidazole-5-*H*), 6.98 (d, *J* = 1.2 Hz, 1H, imidazole-4-*H*), 6.86 (s, 1H, flavone-6-*H*), 6.83 (dd, *J* = 8.6, 2.1 Hz, 1H, flavone-8-*H*), 4.44–4.36 (m, 2H, N-CH_2), 3.43 (t, *J* = 6.4 Hz, 2H, O-CH_2) ppm; ^{13}C NMR (101

MHz, DMSO-d_6) δ: 182.1, 168.4, 166.6, 147.7, 140.1, 132.4, 131.6, 130.3, 129.5, 129.0, 126.0, 123.8, 113.5, 111.4, 68.1, 33.3, 32.4 ppm; MS (m/z): 365 $[M+H]^+$; HRMS (TOF) calcd for $C_{20}H_{16}N_2O_3S$: $[M+H]^+$, 365.0960; found, 365.0962.

*4.2.10. Synthesis of 7-(4-((1H-imidazol-2-yl)thio)butoxy)-2-phenyl-4H-chromen-4-one (**7b**)*

Compound **7b** was prepared according to the experimental procedure for compound **5a**. Yellow solid; Yield: 57%; mp: 199–201 ℃; IR (KBr, cm^{-1}) ν: 3455 (NH), 3061 (Ar–H), 1815 (aromatic frame), 1750 (C=O), 1624, 1555, 1482 (aromatic frame); ^{1}H NMR (400 MHz, DMSO-d_6) δ: 8.02–7.95(m, 2H, Ph-2,6-2*H*), 7.77 (d, *J* = 8.2 Hz, 1H, flavone-5-*H*), 7.58–7.47 (m, 3H, Ph-3,4,5-3*H*), 7.25 (d, *J* = 1.6 Hz, 1H, flavone-3-*H*), 7.20 (d, *J* = 2.4 Hz, 1H, imidazole-5-*H*), 6.96 (d, *J* = 1.6 Hz, 1H, imidazole-4-*H*), 6.85 (s, 1H, flavone-6-*H*), 6.65 (dd, *J* = 8.4, 2.5 Hz, 1H, flavone-8-*H*), 4.45–4.31 (m, 2H, N-CH_2), 3.45 (t, *J* = 6.2 Hz, 2H, O-CH_2), 2.05 (m, 2H, CH_2), 1.98 (m, 2H, CH_2) ppm; ^{13}C NMR (101 MHz, DMSO-d_6) δ: 183.4, 169.3, 166.4, 147.6, 141.2, 134.3, 132.4, 131.4, 129.8, 129.0, 128.1, 123.6, 114.6, 112.3, 69.7, 33.4, 31.3, 14.3, 11.7 ppm; MS (m/z): 393 $[M+H]^+$; HRMS (TOF) calcd for $C_{22}H_{20}N_2O_3S$: $[M+H]^+$, 393.1273; found, 393.1275.

4.3. PTPs inhibition assay

The PTPs were obtained from Prof. Zhang of Shangxi University and expressed and purified as described previously [22]. The inhibitory effects and kinetics analysis of the azoyl flavonoids against PTPs were measured, using *p*-nitrophenol phosphate (*p*-NPP) as the substrate [23]. Briefly, the assays were performed on a 96-well plate in 20 mM MOPS buffer, pH 7.2, containing 50 mM NaCl. 10 μL of the compound at various concentrations was mixed with PTPs solution (82 μL) for 35 min at 37℃. Then 2 μL of *p*-NPP (0.1 M) substrate was added. After incubation for about 30 min, the assays were terminated by the addition of 6 μL of 2 M NaOH. The released *p*-nitrophenolate ion was determined by measuring the absorbance at 405 nm using microplate reader. The results of non-enzymatic hydrolysis of 2 μL *p*-NPP were compensated by measuring the control without enzyme addition. IC_{50} values were obtained by fitting the concentration-dependent inhibition curves using the Origin program (Origin Lab, Northampton, MA).

The inhibiting kinetic analysis was carried out according to the Lineweaver-Burk plot analysis. Phosphatase activities were measured at a fixed enzyme (PTP1B) concentration (0.2 μmol/L) while concentrations of the substrate (*p*-NPP) and the inhibitor **6a** were varied. The data were fitted using Origin program to generate the Lineweaver-Burk plot.

*4.4. The influence of **6a** on cell viability*

The influence of **6a** on cell viability toward HEK293 cells (which were gifts from Prof. Yang, college of pharmacy, ChongQing Medical University, ChongQing, P. R. China) was determined by using Cell Counting Kit-8 (CCK8, Yeasen Company) based on WST-8 (4-(3-(2-methoxy-4-nitrophenyl)-2-(4-nitrophenyl)-2H- tetraz-ol-3-ium-5-yl)benzene-1,3-disulfonate) reduction assay following literature procedures [24]. The HEK293 cells (5000 cells per well) were seeded into 96-well plates. The cells were then incubated in a culture medium containing compound **6a** with a particular concentration for 24 h. After that, 10 mL of CCK8 was added to each well. After 4 h, the unreacted dye was removed by aspiration. The OD values were spectrophotometrically measured in an ELISA plate reader (model 550, Bio-Rad) at a wavelength of 450 nm. The cell survival was expressed as follows: cell viability = (OD treated/OD control)×100%.

Acknowledgments

This work was partially supported by Natural Science Foundation of the Jiangsu Higher Education Institutions of China (No. 17KJB150041), the practice inovation trainng program projects for the Jiangsu College students (No. 201710324004X, 201710324020Z, 201710324126C).

References

[1] (a) P. Punthasee, A,R. Laciak, A.H. Cummings, K.V. Ruddraraju, S.M. Lewis, R. Hillebrand, H. Singh, J.J. Tanner, K.S. Gates, Covalent allosteric inactivation of protein tyrosine phosphatase 1B (PTP1B) by an inhibitor-electrophile conjugate, Biochemistry 56 (2017) 2051–2060; (b) R. Zhang, R Yu, Q. Xu, X. Li, J. Luo, B Jiang, L. Wang, S. Guo, N. Wu, D. Shi, Discovery and evaluation of the hybrid of bromophenol and saccharide as potent and selective protein tyrosine phosphatase 1B inhibitors, Eur. J. Med. Chem. 134 (2017) 24–33.

[2] (a) R. Ottana, I. Adornato, P. Paoli, G. Lori, A. Nass, G. Wolber, V. Cardile, A.C.E. Graziano, A. Rotondo, R. Maccari, Discovery of 4-[(5-arylidene-4-oxothiazolidin-3-yl)methyl]benzoic acid derivatives active as novel potent allosteric inhibitors of protein tyrosine phosphatase 1B: In silico studies and in vitro evaluation as insulinomimetic and anti-inflammatory agents, Eur. J. Med. Chem. 127 (2017) 840–858; (b) Y. Jia, C. Yuan, L. Lu, M. Zhu, S. Xing, X. Fu, A dioxidovanadium (V) complex of NNO-donor Schiff base as a selective inhibitor of protein tyrosine phosphatase 1B: Synthesis, characterization, and biological activities, Eur. J. Med. Chem. 128 (2017) 287–292.

[3] (a) C. Owen, E.K. Lees, N. Mody, M. Delibegovic, Regulation of growth hormone induced JAK2 and mTOR signalling by hepatic protein tyrosine phosphatase 1B, Diabetes Metab. 41 (2015) 95–101; (b) A.R. Saltiel, C.R. Kahn, Insulin signaling and the regulation of glucose and lipid metabolism, Nature 414 (2001) 799–806; (c) P. Heneberg, Use of protein tyrosine phosphatase inhibitors as promising targeted therapeutic drugs, Curr. Med. Chem. 16 (2009) 706–733.

[4] A.P. Combs, W. Zhu, M.L. Crawley, B. Glass, P. Polam, R.B. Sparks, D. Modi, A. Takvorian, E. McLaughlin, E.W. Yue, Z. Wasserman, M. Bower, M. Wei, M. Rupar, P.J. Ala, B.M. Reid, D. Ellis, L. Gonneville, T. Emm, N. Taylor, S. Yeleswaram, Y. Li, R. Wynn, T.C. Burn, G. Hollis, P.C.C. Liu, B. Metcalf, Potent benzimidazole sulfonamide protein tyrosine phosphatase 1B inhibitors containing the heterocyclic (S)-Isothiazolidinone phosphotyrosine mimetic, J. Med. Chem. 49 (2006) 3774–3789.

[5] V.M. Balaramnavar, R. Srivastava, N. Rahuja, S. Gupta, A.K. Rawat, S. Varshney, H. Chandasana, Y.S. Chhonker, P.K. Doharey, S. Kumar, S. Gautam, S.P. Srivastava, R.S. Bhatta, J.K. Saxena, A.N. Gaikwad, A.K. Srivastava, A.K. Saxena, Identification of novel PTP1B inhibitors by pharmacophore based virtual screening, scaffold hopping and docking, Eur. J. Med. Chem. 87 (2014) 578–594.

[6] T.N. Doman, S.L. McGovern, B.J. Witherbee, T.P. Kasten, R. Kurumbail, W.C. Stallings, D.T. Connolly, B.K. Shoichet, Molecular docking and high-throughput screening for novel inhibitors of protein tyrosine Phosphatase-1B, J. Med. Chem. 45 (2002) 2213–2221.

[7] (1) X. Fan, N.J. Xu, J.G. Shi, Bromophenols from the red AlgaRhodomela-confervoides, J. Nat. Prod. 66 (2003) 455–458; (2) J. Luo, Q. Xu, B. Jiang, R. Zhang, X. Jia, X. Li, L. Wang, C. Guo, N. Wu, D. Shi, Selectivity, cell permeability and oral availability studies of novel bromophenol derivative HPN as protein tyrosine phosphatase 1B inhibitor, Brit. J. Pharmaco. 175 (2018) 140–153.

[8] T. Uno, H. Kondo, Y. Inoue, Y. Kawahata, M. Sotomura, K. Iuchi and G. Tsukamoto, Synthesis of antimicrobial agents. 3. Syntheses and antibacterial activities of 7-(4-hydroxypiperazin-1-yl) quinolones, J. Med. Chem. 33 (1990) 2929–2932.

[9] (a) H.A. Jung, M.Y. Ali, H.K. Bhakta, B.S. Min, J.S. Choi, Prunin is a highly potent flavonoid from Prunus davidiana stems that inhibits protein tyrosine phosphatase 1B and stimulates glucose uptake in insulin-resistant HepG2 cells, Arch. Pharm. Res. 40 (2017) 37–48; (b) P.H. Nguyen, T.T. Dao, J. Kim, D.T. Phong, D.T. Ndinteh, J.T. Mbafor, W.K. Oh, New 5-deoxyflavonoids and their inhibitory effects on protein tyrosine phosphatase 1B (PTP1B) activity, Bioorg. Med. Chem. 19 (2011) 3378–3383.

[10] W. Li, S. Li, K. Higai, T. Sasaki, Y. Asada, S. Ohshima, K. Koike, Evaluation of licorice flavonoids as protein tyrosine phosphatase 1B inhibitors, Bioorg. Med. Chem. Lett. 23 (2013) 5836–5839.

[11] S.W. Mao, L. Shuai, H.B. He, N Pan, L.X. Gao, L.F. Yu, J. Li, J.Y. Li, F. Yang, Synthesis and biological evaluation of novel 2,3-pyrazole ring-substituted-4,4-dimethyl lithocholic acid derivatives as selective protein tyrosine phosphatase 1B (PTP1B) inhibitors with cellular efficacy, RSC Adv. 5 (2015) 106551–106560.

[12] T.R. Helgren, R.J. Sciotti, P. Lee, S. Duffy, V.M. Avery, O. Igbinoba, M. Akoto, T.J. Hagen, The synthesis, antimalarial activity and CoMFA analysis of novel aminoalkylated quercetin analogs, Bioorg. Med. Chem. Lett. 25 (2015) 327–332.

[13] B.W. Li, F.H. Zhang, E. Serrao, H. Chen, T.W. Sanchez, L.M. Yang, N. Neamati, Y.T. Zheng, H. Wang, Y. Q. Long, Design and discovery of flavonoid-based HIV-1 integrase inhibitors targeting both the active site and the interaction with LEDGF/p75, Bioorg. Med. Chem. 22 (2014) 3146–3158.

[14] Y. Li, Y. Yu, K. Jin, L. Gao, T. Luo, L. Sheng, X, Shao, J. Li, Synthesis and biological evaluation of novel thiadiazole amides as potent Cdc25B and PTP1B inhibitors, Bioorg. Med. Chem. Lett. 24 (2014) 4125–4128.

[15] J.B. Liu, F.Q. Jiang, Y. Jin, Y. Zhang, J. Liu, W. Liu, L. Fu, Design, synthesis, and evaluation of 2-substituted ethenesulfonic acid ester derivatives as protein tyrosine phosphatase 1B inhibitors, Eur. J. Med. Chem. 57 (2012) 10–20.

[16] J.X. Ong, C.W. Yap, W.H. Ang, Rational design of selective organoruthenium inhibitors of protein tyrosine phosphatase 1B, Inorg. Chem. 51 (2012) 12483–12492.

[17] H.Z. Zhang, G.LV. Damu, G.X. Cai, C.H. Zhou, Design, synthesis and antimicrobial evaluation of novel benzimidazole type of Fluconazole analogues and their synergistic effects with Chloromycin, Norfloxacin and Fluconazole, Eur. J. Med. Chem. 64 (2013) 329–344.

[18] W. Luo, Y. Chen, T. Wang, C. Hong, L.P. Chang, C.C. Chang, Y.C. Yang, S.Q. Xie, C.J. Wang, Design, synthesis and evaluation of novel 7-aminoalkyl-substituted flavonoid derivatives with improved cholinesterase inhibitory activities, Bioorg. Med. Chem. 24 (2016) 672–680.

[19] S.Y. Li, X.B. Wang, S.S. Xie, N. Jiang, K.D. Wang, H.Q. Yao, H.B. Sun, L.Y. Kong, Multifunctional tacrine-flavonoid hybrids with cholinergic, β-amyloid-reducing, and metal chelating properties for the treatment of Alzheimer's disease, Eur. J. Med. Chem. 69 (2013) 632–646.

[20] Y.G. Zheng, M. Zheng, X. Ling, Y. Liu, Y.S. Xue, L.A., N. Gu, M. Jin, Design, synthesis, quantum chemical studies and biological activity evaluation of pyrazole-benzimidazole derivatives as potent Aurora A/B kinase inhibitors, Bioorg. Med. Chem. Lett. 23 (2013) 3523–3530.

[21] E.P. Jesudason, S.K. Sridhar, E.J. Malar, P. Shanmugapandiyan, M. Inayathullah, V. Arul, D. Selvaraj, R. Jayakumar, Synthesis, pharmacological screening, quantum chemical and in vitro permeability studies of N-Mannich bases of benzimidazoles through bovine cornea, Eur. J. Med. Chem. 44 (2009) 2307–2312.

[22] (a) X.L. Li, T. Kurtán, J.C. Hu, A. Mándi, J. Li, X.W. Li, Y.W. Guo, Structural and stereochemical studies of laurokamurols A-C, uncommon bis-sesquiterpenoids from the Chinese red alga laurencia okamurai Yamada, J. Agric. Food Chem. 65 (2017) 1550−1555; (b) L. Ma, L.P. Lu, M.L. Zhu, Q.M. Wang, Y. Li, S. Xing, X.Q. Fu, Z.Q. Gao, Y.F. Dong, Mononuclear copper(ii) complexes with 3,5-substituted-4-salicylidene-amino-3,5-dimethyl-1,2,4-triazole: synthesis, structure and potent inhibition of protein tyrosine phosphatases, Dalton Trans. 40 (2011) 6532−6540.

[23] Q.M. Wang, L.P. Lu, C.X. Yuan, K. Pei, Z.W. Liu, M.L. Guo, M.L. Zhu, Potent inhibition of protein tyrosine phosphatase 1B by copper complexes: implications for copper toxicity in biological systems, Chem. Commun. 46 (2010) 3547−3549.

[24] J.E. Frith, D.J. Menzies, A.R. Cameron, P. Ghosh, D.L. Whitehead, S. Gronthos, A.C.W. Zannettino, J.J. Cooper-White, Effects of bound versus soluble pentosan polysulphate in PEG/HA-based hydrogels tailored for intervertebral disc regeneration, Biomaterials 35 (2014) 1150−1162.

- ► Prepared azolyl flavonoids gave anti-PTP1B activity at the micromolar range.
- ► Compound **6a** (IC_{50} = 1.6 μM) displayed 9.9-fold selectivity for PTP1B over TCPTP.
- ► Cell viability assays indicate **6a** has lower cytotoxicity.
- ► Molecular modeling and dynamics studies reveal the reason of selectivity.

Design, Synthesis of Novel Azolyl Flavonoids and Their Protein Tyrosine Phosphatase-1B Inhibitory Activities

Ling Zhang[1,*], Yu Ge[1], Hao Ming Song[1], Qing Ming Wang[1,*] and Cheng-He Zhou[2]

[1,*] *School of Pharmacy, Yancheng Teachers' University, Yancheng, Jiangsu 224051, People's Republic of China.*

[2] *Laboratory of Bioorganic & Medicinal Chemistry, School of Chemistry and Chemical Engineering, Southwest University, Chongqing, 400715, P.R. China*

Triazolyl flavonoid **6a** displayed the best inhibitory activity (IC_{50} = 1.6 μM) with good selectivity for PTP1B over TCPTP. Cell viability assays indicate **6a** is cell permeable with lower cytotoxicity. Molecular modeling and dynamics studies reveal the reason of selectivity for PTP1B over TCPTP.

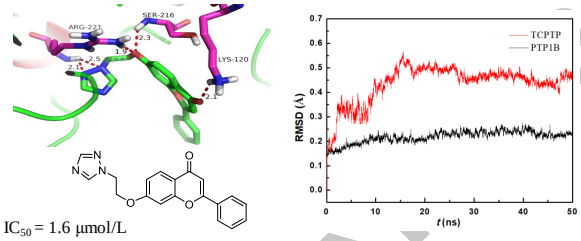

IC_{50} = 1.6 μmol/L